Macromolecules

Volume 31, Number 15 July 28, 1998

Ethene−Norbornene Copolymerization Using Homogenous Metallocene and Half-Sandwich Catalysts: Kinetics and Relationships between Catalyst Structure and Polymer Structure. 1. Kinetics of the Ethene−Norbornene Copolymerization Using the [(Isopropylidene)(η^5-inden-1-ylidene-η^5-cyclopentadienyl)]zirconium Dichloride/Methylaluminoxane Catalyst

Dieter Ruchatz and Gerhard Fink*

Max-Planck-Institut für Kohlenforschung, Kaiser-Wilhelm-Platz 1,
45470 Mülheim an der Ruhr, Germany

Received July 15, 1997; Revised Manuscript Received April 22, 1998

ABSTRACT: The kinetics of the ethene−norbornene copolymerization using the [(isopropylidene)(η^5-inden-1-ylidene-η^5-cyclopentadienyl)]zirconium dichloride (^{i}Pr[IndCp]ZrCl$_2$)/methylaluminoxane catalyst has been investigated at 70 °C in a concentrated solution of norbornene in toluene and an ethene pressure ranging from 4 to 60 bar (58−870 psi). The ethene reaction rate has been measured during the copolymerization process at varying reactant concentrations. The reaction orders and rate constants were determined and compared to the corresponding values of the ethene and norbornene homopolymerizations. It was found that $k_E^{homo} > k_E^{co}$ and $k_N^{homo} < k_N^{co}$. The copolymerization parameters are $r_1 = 0.9$ and $r_2 = 0.05$.

Introduction

A few years after the discovery of the Ziegler catalysts, attempts were made to polymerize cycloolefins.[1−6] The processes, developed prior to 1984 and based on heterogeneous Ti or V catalysts, had many disadvantages. These disadvantages included low activities and varying product properties that were difficult to control. A breakthrough was finally achieved with metallocene/methylaluminoxane (MAO) catalysts.[7−10] The polymerization of, for example, cyclopentene or norbornene using metallocenes yields crystalline, insoluble polymers with high temperature and chemical resistance. The reason for the high stability of polycycloolefins is that the polymerization of norbornene proceeds exclusively by opening the double bond and not by a ring-opening metathesis reaction with the formation of the unsaturated, thermally unstable poly(1,3-cyclopentenevinylene) (Figure 1).

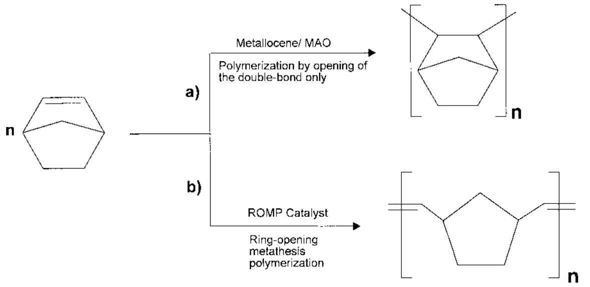

Figure 1. Possible polymerization reactions of norbornene.

Polycycloolefins produced with metallocene catalysts show no melting point. They cannot be processed like thermoplastic polymers and therefore they are of no commercial interest. Ethene−cycloolefin copolymers, however, do show thermoplastic behavior together with other interesting properties:[8−15] e.g., ethene−norbornene copolymers are armophous, highly transparent, and chemically resistant (Figure 2). For these reasons, the ethene−norbornene copolymers belong to a new class of technical thermoplastics for high-quality applications. The main advantage of these copolymers lies in their wide-ranging glass transition temperatures, which can be set from 20 to 260 °C by varying the norbornene content in the copolymer. Furthermore, the distribution

S0024-9297(97)01041-3 CCC: $15.00

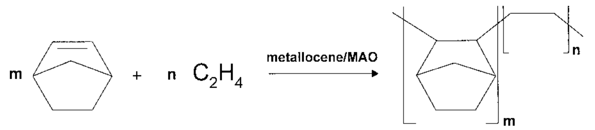

Figure 2. Ethene–norbornene polymerization with metallocene–MAO catalysts.

of the monomers in the copolymer can be controlled from statistical to alternating.[14] Due to the absence of polar, unsaturated, or aromatic groups and their high transparency, the applications of ethene–norbornene copolymers include the production of compact discs, optical lenses, and light-conducting fibers. Their high temperature resistance makes them suitable for molded articles for thermally stressed applications.

The specific control of the polymer microstructure in the metallocene-catalyzed olefin polymerization, especially in the case of the propene polymerization, by varying the catalyst structure is well examined and understood.[16–18] The investigations concerning the olefin copolymerization have been less intensive. The aim of this work has been the study of the influence of different metallocene/MAO catalysts on the microstructure of ethene–norbornene copolymers. In addition some halfsandwich catalysts ("constrained geometry catalysts") were used for the first time in ethene–cycloolefin copolymerization.

The copolymerizations were carried out at 70 °C and ethene pressures ranging from 4 to 60 bar (58–870 psi) in a concentrated solution of norbornene in toluene. A special polymerization reactor with catalyst solution injection system (in situ start) and gas flow meters were used for kinetic measurements covering the entire pressure range.

Experimental Section

All operations were carried out under an argon atmosphere.

Materials. Ethene (Messer-Griesheim) was dried over molecular sieves, 3 Å, and sodium tetraethylaluminate (NaAlEt$_4$). Toluene was predried over Na/K alloy, subsequently dried over NaAlEt$_4$, and then distilled. Norbornene (Fluka) was distilled, dissolved in dried toluene (85 vol % norbornene), and purified over dried aluminum oxide (Kompalox, Martinswerke). MAO (10 wt % solution in toluene) was purchased from Witco. The ^{i}Pr[IndCp]ZrCl$_2$ catalyst was synthesized according to the literature;[19] the complex purity (>99%) was checked by ^{1}H NMR and MS before use.

Polymerizations. All copolymerizations were carried out in a 1 L steel autoclave (Büchi) with stirrer (800 rpm) at constant ethene pressure in a concentrated solution of norbornene in toluene (norbornene concentration 7.4 mol/L). MAO was added to the norbornene solution and filled into the carefully dried reactor. The solution (total volume = 0.40 L) was heated to 70 °C and saturated with ethene. The high-pressure injection system was filled with the preactivated ^{i}Pr[IndCp]ZrCl$_2$/MAO solution, which was injected into the reactor with an argon overpressure. The ethene consumption was measured with thermal mass flowmeters (Brooks Instrument) and together with the reaction temperature was registered on a recorder. At low reaction conversions (<5% norbornene; polymerization time 20 min) the polymerization was stopped by rapidly cooling the reaction mixture and carefully venting off the ethene pressure. The reaction mixture was poured into 4 L of acetone and the unsoluble polymer was stirred overnight, filtered, and then again stirred in 4 L of fresh acetone. The product was filtered and then dried in a vacuum oven at 70 °C and 10 mbar for at least 18 h.

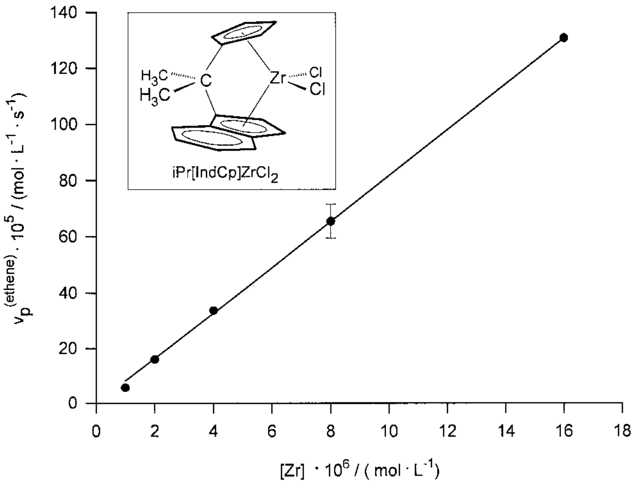

Figure 3. Ethene reaction rate vs Zr concentration. Polymerization conditions: [Al]/[Zr] = 4525; [ethene] = 2.44 mol L^{-1} (20 bar); [norbornene] = 7.4 mol L^{-1}; T = 70 °C.

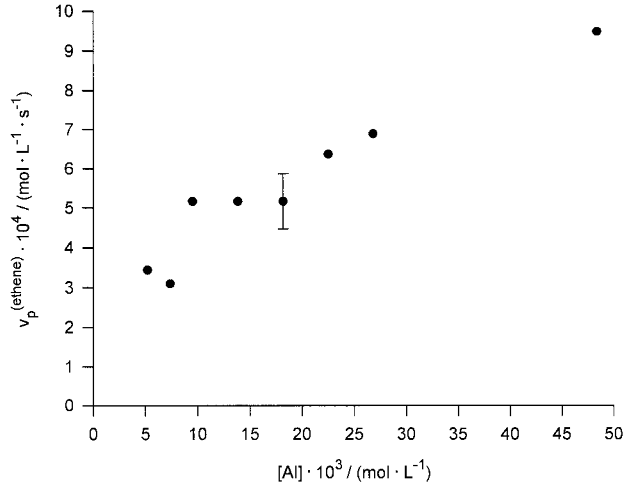

Figure 4. Ethene reaction rate vs [Al]/[Zr]. Polymerization conditions: [Zr] = 2.6 × 10^{-5} mol L^{-1}; [ethene] = 2.6 mol L^{-1} (p = 21.5 bar); [norbornene] = 7.4 mol L^{-1}; T = 50 °C.

Results

The following results were obtained with the ^{i}Pr[IndCp]ZrCl$_2$/MAO catalyst. The influence of the Zr concentration on the ethene reaction rate was measured in the range of 1.0 × 10^{-6} to 1.6 × 10^{-5} mol L^{-1}: Figure 3 shows a linear relationship between Zr concentration and ethene reaction rate. From the rate law $v_P^{ethene} = k_E[Zr][ethene]$ the rate constant for ethene k_E was calculated to be $k_E = 34$ L mol^{-1} s^{-1}. The reaction order for Zr is first order.

The measurement of the ethene reaction rate dependence on the MAO concentration was problematic in the beginning. At low MAO concentrations ([Al] < 4.8 × 10^{-3} mol L^{-1} = [Al]/[Zr] ≈ 690), the polymerization activity dropped rapidly toward zero. This behavior is possibly caused by impurities. MAO can be consumed by impurities due to its scavenging behavior. To overcome this effect at low [Al]/[Zr] values, the Zr concentration was increased, which increased the aluminum concentrations to acceptable levels. As a consequence of the high catalyst concentration, the polymerization activities were very high and the measurement of ethene consumption was difficult. Therefore, the polymerization temperature was reduced from the normal 70 °C to 50 °C. The results of this series of

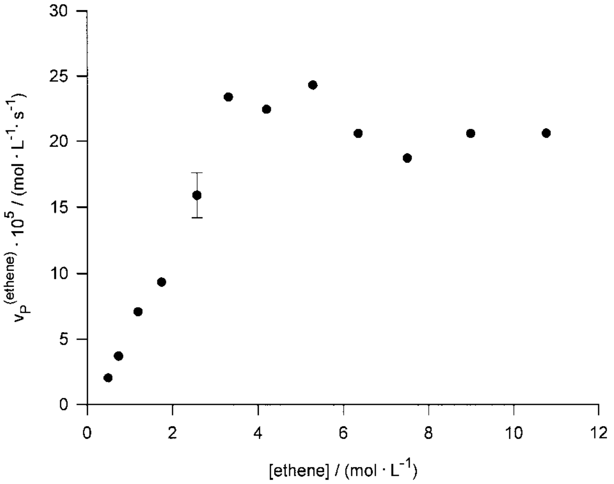

Figure 5. Ethene reaction rate vs ethene concentration (pressure 4−55 bar). Polymerization conditions: $[Zr] = 2.00 \times 10^{-6}$ mol L^{-1}; [Al]/[Zr] = 4525; [norbornene] = 7.4 mol L^{-1}; $T = 70$ °C.

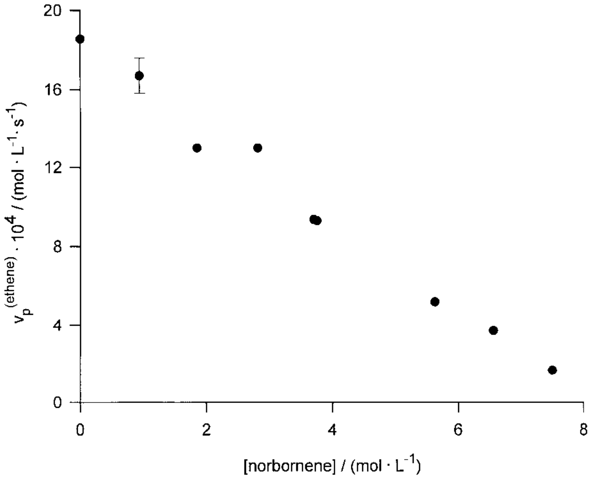

Figure 6. Ethene reaction rate vs norbornene concentration. Polymerization conditions: $[Zr] = 2.00 \times 10^{-6}$ mol L^{-1}; [Al]/[Zr] = 4525; [ethene] = 6.2 mol L^{-1} ($p = 40$ bar); $T = 70$ °C.

measurements are shown in Figure 4. Molar ratios of [Al]/[Zr] from 200 to 2000 were studied. A linear dependence between the ethene reaction rate and the Al concentration were found in this interval. The reaction order for Al was found to be 0.5. In two additional series of measurements, it was found that the ethene reaction rate cannot be further increased by increasing the ratio of [Al]/[Zr]. Even at [Al]/[Zr] molar ratios of 40 000 the reaction rate was not higher than at an [Al]/[Zr] molar ratio of 2000.

The influence of the ethene concentration on the ethene reaction rate is shown in Figure 5: Up to an ethene concentration of 3.5 mol L^{-1} (26 bar) the ethene reaction rate increases linearly. Further increasing of the ethene concentration causes no further increase in the ethene reaction rate.

Analogous to the situation in Figure 3, the low ethene concentration section in Figure 5 (the first six points) was used to calculate the ethene rate constant k_E for the copolymerization with the help of the rate law (see above). The value was found to be $k_E = 30$ L mol^{-1} s^{-1} and is similar to that of the value calculated previously. The ethene reaction order was determined, from the first six points in Figure 5, to be 1.

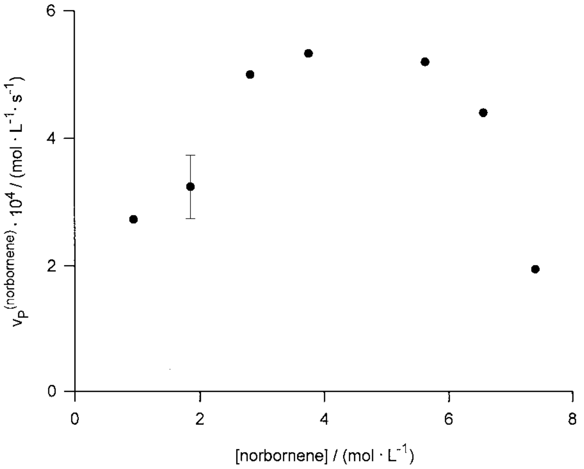

Figure 7. Norbornene reaction rate vs norbornene concentration. Polymerization conditions are as in Figure 6.

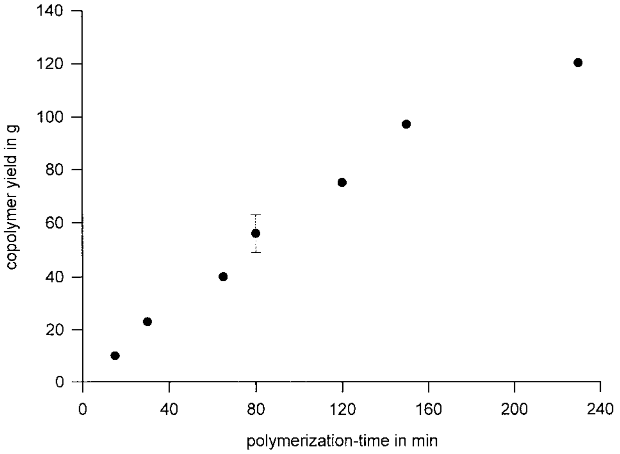

Figure 8. Copolymer yield vs reaction time. Polymerization conditions: $[Zr] = 2.00 \times 10^{-6}$ mol L^{-1} [Al]/[Zr] = 4525; [ethene] = 2.44 mol L^{-1} (20.0 bar); [norbornene] = 7.4 mol L^{-1}; $T = 70$ °C.

The influence of the norbornene concentration on the ethene reaction rate is shown in Figure 6. A linear dependence was found in the entire norbornene concentration range and the ethene reaction rate was found to decrease linearly with increasing norbornene concentrations.

The norbornene reaction rate could not be directly measured, but an average value was calculated by measuring the norbornene content in the copolymers by ^{13}C NMR after a short but known polymerization time and determination of the copolymer yields; the ethene content in the copolymers can be determined from the integrated ethene consumption diagram, which is measured experimentally by the ethene flowmeters. The calculated values for the reaction rate of norbornene are shown in Figure 7: The norbornene reaction rate passes through a maximum.

From the slope of the first four points in Figure 7 and the rate law

$$v_N = k_N[\mathrm{Zr}][\mathrm{norbornene}]$$

the norbornene rate constant can be calculated. A value of $k_N = 80$ L mol^{-1} s^{-1} and a reaction order of 0.5 were found.

A stable catalyst is a basic requirement for its utilization in an industrial production process. To

Table 1. Reaction Orders[a] for Ethene and Norbornene Homopolymerization and Ethene−Norbornene Copolymerization Using the ^{i}Pr[IndCp]ZrCl$_2$/MAO Catalyst

reaction compound	ethene−norbornene copolymerization	ethene homo-polymerization	norbornene homo-polymerization
Zr	1	1	1
Al	0.5 (50 °C)	1 (25 °C)	0.85
ethene	1	1.1; 1.5 (35 °C)	
norbornene	0.5		0.5−0.7

[a] At 70 °C

examine catalyst stability, several copolymerization runs were carried out and stopped after different time intervals. The copolymer yields were determined and are shown in Figure 8. There is a linear increase in the copolymer yield during the first 3 h with no loss of activity. After 4 h of polymerization time, the activity is slightly decreased. This apparent decrease in activity is probably not due to the deactivation of the catalyst but rather is probably due to the increasing viscosity of the reaction mixture. Increased viscosities results in decreased ethene concentrations in the reaction medium due to more difficult absorption of the ethene from the gas phase in the solution.

Discussion

The main results are the following:

(a) The ethene reaction rate v_P^{ethene} decreases linearly with increasing norbornene concentration. In the ethene concentration interval from 0 to 3.5 mol L^{-1} (0−26 bar), v_P^{ethene} increases linearly with increasing ethene concentration. Further increasing of the ethene concentration to 11 mol L^{-1} (60 bar) causes no further increases of the v_P^{ethene}. With increasing norbornene concentration the norbornene reaction rate $\mathrm{v}_P^{\text{Norb}}$ goes through a maximum.

(b) The ethene rate constant of the ethene−norbornene copolymerization, k_E^{co}, is *smaller* than the ethene rate constant of the ethene homopolymerization, k_E^{homo}. In contrast, the norbornene rate constant of the ethene−norbornene copolymerization, k_N^{co}, is *larger* than the norbornene rate constant of the norbornene homopolymerization, k_N^{homo}.

$$k_E^{\text{co}} < k_E^{\text{homo}}$$

$$k_N^{\text{co}} > k_N^{\text{homo}}$$

In Tables 1 and 2 the reaction orders, rate constants, and activation energies of the ethene−norbornene copolymerizations are compared with the corresponding values of the ethene and norbornene homopolymerizations. A detailed discussion together with results for other catalysts studied follows in Part 3 of this series.[20]

From the kinetic results the following conclusions can be drawn: If the growing polymer chain consists exclusively of norbornene, the insertion rate and therefore k_N^{homo} is very low as a result of the steric hindrance of the bulky monomer norbornene and the growing polynorbornene chain. If the norbornene is polymerized together with ethene, the norbornene can be inserted more easily due to sterically less hindered polymer chain ends with the sequence R−(E)$_n$, especially in the case of low norbornene concentrations. The result is a higher norbornene insertion rate in comparison to the norbornene homopolymerization. At higher [norbornene]/[ethene] ratios, the probability for the insertion of the norbornene in the chain end with the sequence R−N increases and a decrease in the norbornene insertion rate results. At low norbornene concentrations, the chain ends with the sequence R−(E)$_n$ are predominant and the norbornene polymerization rate $v_P^{(\text{N,co})}$ increases with increasing norbornene concentration according to the rate law (Figure 7). At high norbornene concentrations the number of the chain ends with the sequence R−N will dominate and at some point overcome the concentration effect. The result is a decrease in $v_P^{(\text{N,co})}$ at high norbornene concentrations due to the above-mentioned steric effects.

Table 2. Rate Constants, Copolymerization Parameters, and Activation Energies for Ethene- and Norbornene Homopolymerization and Ethene−Norbornene Copolymerization Using the ^{i}Pr[IndCp]ZrCl$_2$/MAO Catalyst

	ethene−norbornene Copolymerization	ethene homo-polymerization	norbornene homo-polymerization
k_E (L mol^{-1} s^{-1})	30−34[a,b] 42[a,c]	160[a,b]	
k_N (L mol^{-1} s^{-1})	80[a,c]		1.5[a,c]
r_1;r_2	0.88; 0.05[a]		
E_A^{ethene} (kJ mol^{-1})	155 (60−70 °C) 24 (70−90 °C)	73 (20−80 °C)	
E_A^{norb} (kJ mol^{-1})	128 (60−70 °C) 14 (70−90 °C)		63 (10−100 °C)

[a] At 70 °C. [b] According to ethene flowmeters. [c] According to copolymer yield.

If the rate constants k_E and k_N in Table 2 are to be compared and correctly interpreted, one has to keep in mind that the homopolymerization happens to be the repetition of the same elementary insertion steps as the growing polymer chain end always remains the same. This sequence of identical insertion steps is represented by k^{homo}. In the case of the copolymerization, the insertion steps are represented by k^{co}. But in contrast to k^{homo}, k^{co} is an average value. It is the sum of the rate constants of the different insertion steps of the copolymerization. These insertion steps are known from the definition of the copolymerization parameters; i.e., k_{EE} differs from k_{NE}, etc., as a result of the influence of the last inserted monomer unit on the next insertion step (Markov model first order). However, in the case of metallocene-catalyzed ethene−norbornene copolymerization the Markov model second order seems to be more probable. In this case, the rate constants for the monomer insertion by the copolymerization are defined as follows: $k_E^{\text{co}} = k_{EEE} + k_{NEE} + k_{NNE}$ and $k_N^{\text{co}} = k_{NNN} + k_{ENN} + k_{EEN}$. The homopolymerization rate constants k_E^{homo} and k_N^{homo} can be regarded as a limit for the corresponding values of the ethene−norbornene copolymerization: $k_E^{\text{homo}} \approx k_{EEE}$ and $k_N^{\text{homo}} \approx k_{NNN}$.

On the basis of the rate constants listed in Table 2, theoretical limits of the copolymerization parameter (r') can be calculated. For k_{EE} and k_{NN} the respective rate constant of the homopolymerization, k_E^{homo} and k_N^{homo}, was used; for k_{EN} and k_{NE} the values of the copolymerization k_N^{co} and k_E^{co} were used. The result amounts to the following:

On the basis of the norbornene content in the copolymers, the following values were found: $r_1 = 0.9$ and $r_2 = 0.05$. For r_2' only a range can be given because the values for k_N^{homo} and k_E^{co} could not be measured exactly. The calculated r_1' value $= 3.8$ is higher than the copolymerization parameter $r_1 = 0.9$ which was determined by the Kelen−Tüdös method.[21−23] The upper limit of the calculated interval for r_2' is of the same magnitude as the r_2 copolymerization parameter, which was determined from the Kelen−Tüdös diagram. The differences between r_1' and r_1 as well as r_2' and r_2 are relatively small, although the r' values were calculated with limits or average values: r_1' is higher than r_1 and r_2' is lower than r_2 because the used rate constants k_{EE} and k_{NN} of the homopolymerization for calculating the r' values can be regarded as an upper and lower limit in the copolymerization procedure.

More difficult to explain is the leveling off of the increment of v_P^E with increased ethene concentrations (Figure 5). This effect was observed only with the catalyst $^iPr[IndCp]ZrCl_2$. All other catalysts that were investigated[24] showed an increase in v_P^E covering the entire ethene concentration range.

The result $k_E^{homo} > k_E^{co}$ is due to steric effects of the norbornene units in the growing polymer chain, as has been explained above. In other words, the frequency of insertion depends on the chain end. This well-known behavior can also explain the second result, $k_N^{homo} < k_N^{co}$. The norbornene insertion step works faster if one or more ethene molecules are inserted beforehand; the ethene sequences in the copolymer act like a small spacer between the bulky norbornene units or norbornene sequences. In the case of the norbornene homopolymerization, the insertion step is sterically hindered by the growing polynorbornene chain and, therefore, is much slower than in the copolymerization process with ethene.

References and Notes

(1) DuPont. U.S. Patent 2,721,189, 1954.
(2) Montecatini. German Patent DE 152,0259, 1961.
(3) Montecatini. Bristish Patent GB 951,022, 1961.
(4) VEB Leuna. German Patent DD 109,224, 1973.
(5) VEB Leuna. German Patent DD 222,317, 1984.
(6) Mitsui Petrochemical. European Patent EP 156,464, 1984.
(7) Kaminsky, W.; Spiehl, R. *Makromol. Chem.* **1989**, *190*, 515.
(8) Kaminsky, W.; Bark, A.; Däke, I. In *Catalytic Olefin Polymerization*; Soga, K., Keii, T., Eds.; Kodansha: Tokyo, 1990.
(9) Kaminsky, W.; Bark, A.; Arndt, M. *Makromol. Chem., Macromol. Symp.* **1991**, *47*, 83−93.
(10) Kaminsky, W.; Bark, A.; Steiger, R. *J. Mol. Catal.* **1992**, *74*, 109.
(11) Kaminsky, W.; Bark, A. *Polym. Int.* **1992**, *28*, 251.
(12) Kaminsky, W.; Noll, A. *Polym. Bull.* **1993**, *31*, 175.
(13) Kaminsky, W.; Noll, A. In *Ziegler Catalysts, Recent Scientific Innovations and Technological Improvements*; Fink, G., Mülhaupt, R., Brintzinger, H.-H., Eds.; Springer: Berlin, Heidelberg, and New York, 1995.
(14) Cherdron, H.; Brekner, M.-J.; Osan, F. *Angew. Makromol. Chem.* **1994**, *223*, 121.
(15) Land, H.-T.; Niedernberg, D. *Kunststoffe* **1995**, *85*, 8.
(16) van der Leek, Y.; Angermund, K.; Reffke, M.; Kleinschmidt, R.; Goretzki, R.; Fink, G. *Chem. Eur. J.* **1997**, *3*, 585.
(17) Fink, G.; Mülhaupt, R.; Brintzinger, H.-H. *Ziegler Catalysts, Recent Scientific Innovations and Technological Improvements*, Springer: Berlin, Heidelberg, and New York, 1995.
(18) Brintzinger, H. H.; Fischer, D.; Mülhaupt, R.; Rieger, B.; Waymouth, R. *Angew. Chem.* **1995**, *107*, 1255.
(19) Spaleck, W.; Antberg, M.; Dolle, V.; Klein, R.; Rohrmann, J.; Winter, A. *New J. Chem.* **1990**, *14*, 499.
(20) Ruchatz, D.; Fink, G. *Macromolecules* **1998**, *31*, 4681−4683 (third of four papers in this issue).
(21) Kelen, T.; Tüdös, F. *J. Macromol. Sci.-Chem.* **1975**, *A9*, 1.
(22) Kelen, T.; Tüdös, F. *J. Polym. Sci., Polym. Chem. Ed.* **1975**, *13*, 2277.
(23) Kelen, T.; Tüdös, F. *Reaction Kinet. and Catal. Letter* **1974**, *1* (4), 487.
(24) Ruchatz, D.; Fink, G. *Macromolecules* **1998**, *31*, 4674−4680 (second of four papers in this issue).

MA971041R